Available online at www.sciencedirect.com

ScienceDirect

Procedia Structural Integrity 52 (2024) 523–534

Structural Integrity Procedia

www.elsevier.com/locate/procedia

Fracture, Damage and Structural Health Monitoring

Investigation on the Low Cycle Thermal Fatigue of a Hybrid Power Unit Transmission Clutch

Saverio Giulio Barbieri[a]*, Valerio Mangeruga[a], Andrea Piergiacomi[a], Matteo Giacopini[a]

[a]*University of Modena and Reggio Emilia, Engineering Department "Enzo Ferrari", via Vivarelli 10, Modena (MO) 41125, Italy*

Abstract

A numerical methodology for the thermal-structural assessment of a clutch for a high-performance hybrid power unit is proposed. Clutches are commonly adopted in internal combustion engines to connect the crankshaft to the gearbox. However, the specific clutch under investigation is employed for the coupling between the electric motor and the engine transmission primary shaft in a P2 hybrid architecture. In this specific configuration, the clutch may be activated and deactivated frequently to maximise the efficiency of the power unit depending on the required output torque and on the particular control strategy developed. As a consequence, the thermal loads insisting on the clutch may differ with respect to the ones encountered in a typical full combustion architecture. The results of the presented research show the great influence of the thermal deformation on the stress state of this component, and the onset of possible failure due to low cycle fatigue phenomena is detected. In addition, the influence of different modelling strategies is considered.

Keywords: low cycle fatigue; thermal fatigue; hybrid power unit; transmission clutch

Nomenclature

E_{tot}	total energy generated by friction
EM	electric motor
FE	Finite Element
HTC_{air}	heat transfer coefficient with the surrounding air
ICE	internal combustion engine
Mt_2	torque of the EM

* Corresponding author. Tel.: +39-059-205-6163.
E-mail address: saveriogiulio.barbieri@unimore.it

2452-3216
10.1016/j.prostr.2023.12.052

$\dot{Q}$	thermal power
$\dot{Q}_{av}$	average thermal power
c	damage sensitivity coefficient
k_{air}	thermal conductivity of air
$\Delta speed$	difference between the revving speed of the ICE and the one of the EM
$speed_1$	revving speed of the ICE
$speed_2$	revving speed of the EM
t_{cycle}	duration of one cycle of the clutch
γ	back-stress coefficient
υ_{air}	kinematic viscosity of air

1. Introduction

Traditionally, automotive clutches have the task of properly connecting and disconnecting the crankshaft and the gearbox of an internal combustion engine (Steinhagen 1980; Della Gatta et al. 2018). In this context, the frequency of the engagements is moderate, and the heat generated by unavoidable slippages is rarely responsible for damaging the clutch (Foulard et al. 2015; Sivanesan et al. 2017). In hybrid electric motor (EM)/internal combustion engine (ICE) configurations, the clutch usage is influenced by the specific power unit control strategy adopted, with the aim of optimizing energy consumption (Minh et al. 2012). In particular, in P2 architectures such as the one examined in the present contribution, the clutch is installed between the internal combustion engine and the electric motor (Wang et al. 2016). This design strategy has the advantage of connecting and disconnecting the EM and the ICE at will, thus allowing the power unit to run even in a full electric configuration.

In the following, the main strategies for using a P2 architecture hybrid power unit are briefly analysed. First, the configurations used to exploit the energy stored in the fuel tank and the battery pack are considered. When the clutch is engaged, the EM and the ICE are connected. In this case, it is possible to obtain the maximum power; the whole power unit transmits motion to the wheels. If the friction is disengaged, only the EM can transmit power. This configuration is used when the power required is lower than the maximum power that can be supplied by the entire power unit and when the battery is sufficiently charged to supply the needed energy. In general, when intermediate power is required or when the internal combustion engine is employed to recharge the batteries, the clutch is engaged. Then, the braking phase is briefly considered. When the vehicle has to be slowed down, the clutch can be disengaged and thus the speed of the vehicle can be reduced by fully exploiting the inertia of the vehicle to charge the batteries. In addition, to maximize the braking effect, it is possible to engage the clutch to also use the internal combustion engine to dissipate energy parallel to the operation of the electric motor thus saving the disc brakes.

From this brief analysis, the utility of a P2 hybrid configuration and the degrees of freedom it adds to power transmission control are undisputed, even if very frequent use of the clutch is unavoidable. Furthermore, the higher the efficiency required, the more frequency the clutch is used. When the clutch is disengaged, the relative revving speeds between the upstream (ICE side) and downstream (EM side) of the clutch are generally different and when the clutch is engaged, the lack of synchronization between the various clutch plates causes short but intense micro slips which generate heat for friction (Ivanović et al. 2009; Abdullah et al. 2019). Commonly, the heat generated by friction has time to be dissipated in clutches for traditional ICEs. In P2 hybrid power units, the activations are much more frequent. Consequently, the geometries of the components involved, and the strategies of use must be able to disperse the greater accumulated heat to avoid reaching harmful temperatures and related thermal-structural stresses (Afferrante et al. 2004).

In the present study, a hybrid power unit specifically designed for Formula SAE application is considered (Mangeruga et al. 2019; Mattarelli et al. 2019). The first version, currently installed on the racing vehicle and running, exploits a P0 configuration (Pavković et al. 2022) and therefore the electric motor and the internal combustion engine are permanently connected through a transmission chain (Mangeruga et al. 2020, 2023 a; b). To include the aforementioned advantages of a P2 configuration, a second solution for the power unit has been designed, where a motorcycle clutch has been inserted between the internal combustion engine and the transmission chain thus having the possibility of decoupling the ICE and the EM. Unfortunately, the evidence of the first bench

tests revealed the onset of damage on the clutch discs responsible for the transmission of motion. Since the registered number of cycles to failure has been much less than a thousand, phenomena of low cycle fatigue and, in particular, thermal-structural fatigue, have been supposed to be responsible for the fracture and thus investigated (Charkaluk et al. 2003; Constantinescu et al. 2004; Lorenzini et al. 2018; Barbieri et al. 2023).

This contribution illustrates a Finite Element (FE) methodology to explain these breakages and the thermal-mechanical phenomena that cause them.

The paper is organized as follows. In Section 2, the layout of the power unit, the geometry of the components taken into analysis, the location where the failure is detected, and the main material properties are illustrated. Section 3 examines the bench tests and explains how the boundary conditions to be applied to the FE models are derived. Section 4 presents the FE models prepared in increasing order of complexity and the obtained results are discussed. The conclusions of Section 5 end the contribution.

2. The layout of the hybrid driveline, the geometry and the material properties of the components involved in the analysis

Fig. 1 depicts the layout of the P2 hybrid driveline. The clutch investigated in this paper is installed between the ICE and the EM. Points 1 and 2 indicate the locations where the sensors have been placed to monitor the revving speed and the torque.

Fig. 2 (a) and (b) display the simplified CAD file of the clutch. Only the components directly involved in the thermal-structural analysis have been modelled. In particular, three friction plates, the pressure plate, two steel plates, the spline profiled shaft, the clutch basket and the flywheel are visible. The so-called friction disc has been the main focus of the analysis and, therefore, it has been modelled following the actual component faithfully. The friction plate is an assembly consisting of the structural disc, the friction material applied on the periphery of the structural disc and the spline profiled disc linked to the structural disc by rivets. The structural disc has multiple and contrasting purposes. On one side, it has to be stiff and resistant to transmit the torque between the two sides of the clutch. On the other hand, it has to be flexible to permit the friction material to be in contact with the pressure plate, the steel plates and the flywheel despite the unavoidable deformation due to both mechanical and thermal loadings. Moreover, the structural disc has to be as light as possible to limit its inertial contribution and not jeopardize the global performance of the power unit. As a result of these opposing aims, Fig. 2 (c) displays how the geometry of the structural disc is rich in lightening features and notches. The red line in Fig. 2 (c) shows the location and the crack propagation evidenced during the experiments and the specific nucleation point (Point A).

Moving to Table 1, the properties of the materials employed are collected. The steel AISI 1060 has been employed for all the components involved in the analysis except for the friction surfaces, where a specific friction material has been selected. The mechanical properties of the AISI 1060 have been implemented in the FE model as a function of temperature; in particular, the Chaboche formulation has been adopted (Chaboche 1986, 1989, 2008) for the non-linear kinematic hardening modelling, see Fig. 3. Instead, the properties of the friction material do not exhibit a substantial variation in the range of temperature commonly encountered in this application.

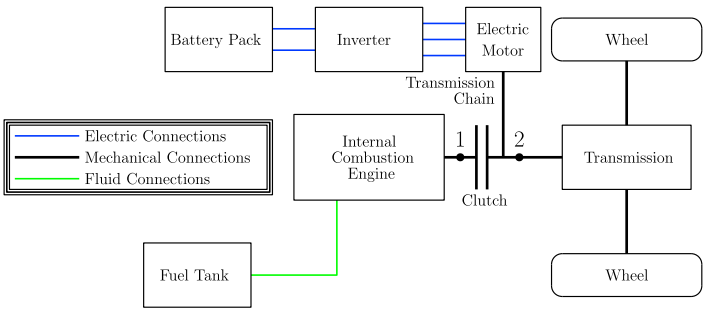

Fig. 1. The layout of the hybrid driveline.

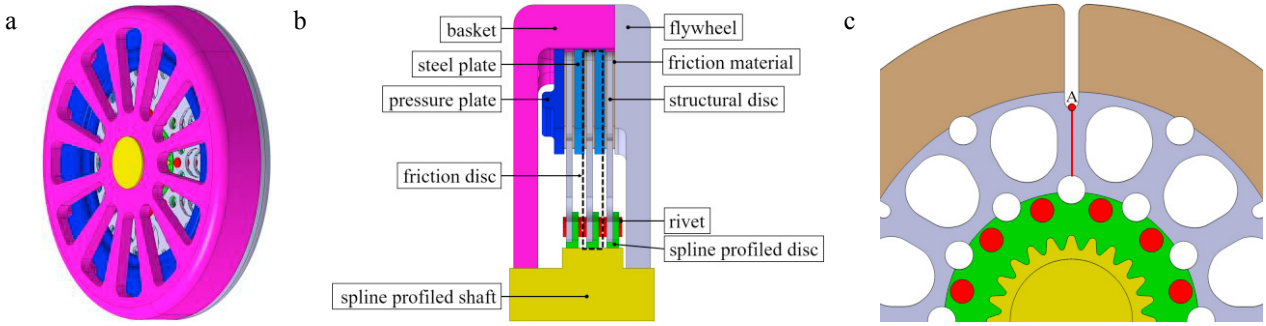

Fig. 2. Simplified CAD file of the clutch: (a) isometric view; (b) sectional view; (c) detail of the friction disc.

Table 1. Material properties.

AISI 1060	
Density	7.9 kg/dm^3
Conductivity	0.04 W/(mm°C)
Specific heat	460 J/(Kg°C)
Young's modulus	Function of temperature
Poisson's ratio	0.3
Thermal expansion	$1.2 \cdot 10^{-5}$
Plasticity	Function of temperature
Friction material	
Density	5.25 kg/dm^3
Conductivity	0.03 W/(mm°C)
Specific heat	550 J/(Kg°C)
Young's modulus	5.2 GPa
Poisson's ratio	0.3
Thermal expansion	$1.5 \cdot 10^{-6}$
Plasticity	Not considered

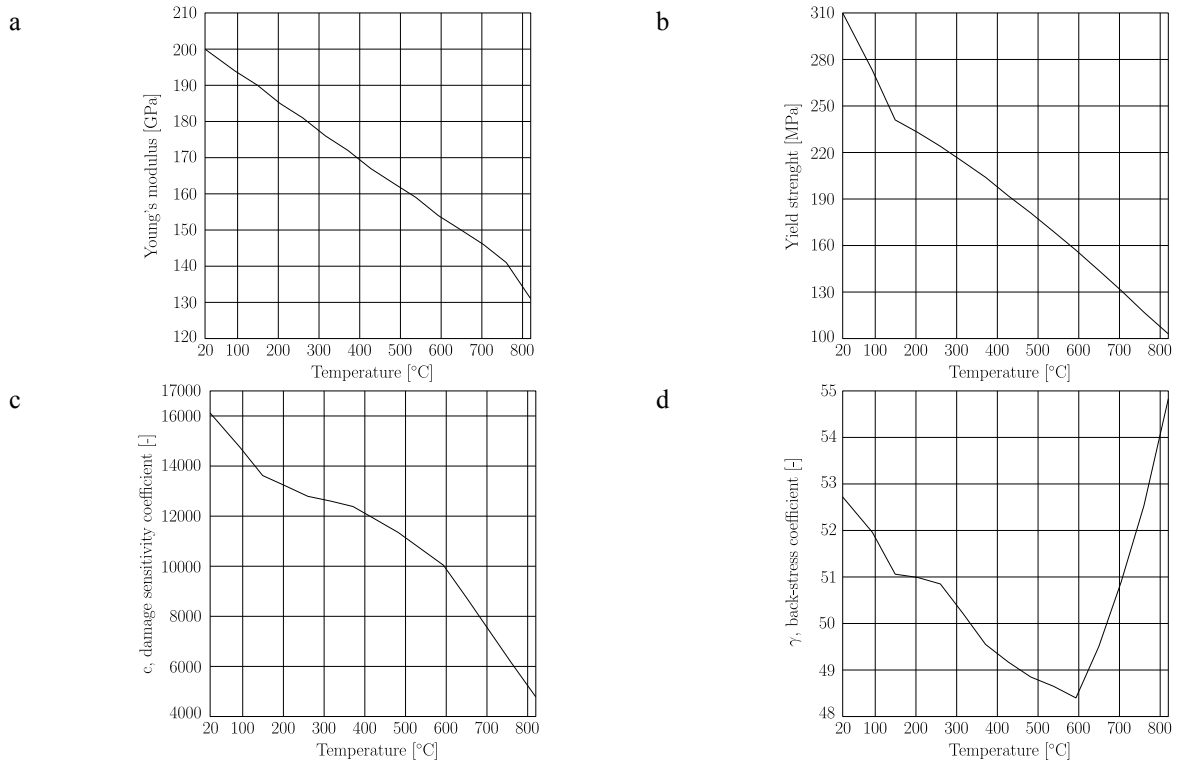

Fig. 3. Properties of AISI 1060 as a function of temperature: (a) Young's modulus; (b) yield strength; (c) c, damage sensitivity coefficient; (d) γ, back-stress coefficient.

3. Estimation of the boundary conditions

The thermal structural methodology proposed requires the definition of both thermal and structural boundary conditions. The formers have been estimated from the analysis of the velocity and torque before and after the clutch (see points 1 and 2 of Fig. 1). The letters have consisted of the force applied by the spring to the pressure plate and the centrifugal force based on the regime revving speed of the clutch. The effect of the instantaneously transmitted torque has been neglected since preliminary thermal-mechanical calculations have shown its contribution is marginal in terms of low-cycle fatigue phenomena.

Two thermal boundary conditions have been applied: the heat flux generated by friction and micro slips, and heat exchange with the surrounding air while the clutch is moving.

The heat produced by friction has been estimated by analyzing the revving speed of the shaft on the side of the ICE (point 1), and the revving speed and the torque on the side of the EM (point 2). These quantities have been recorded during the bench tests. The clutch has been engaged and disengaged several times and only one cycle of the duration of 20s has been depicted in Fig. 4 since the repeated cycles have exhibited almost the same trend. The following formulation has been employed to estimate the profile of the thermal power generated during the cycles.

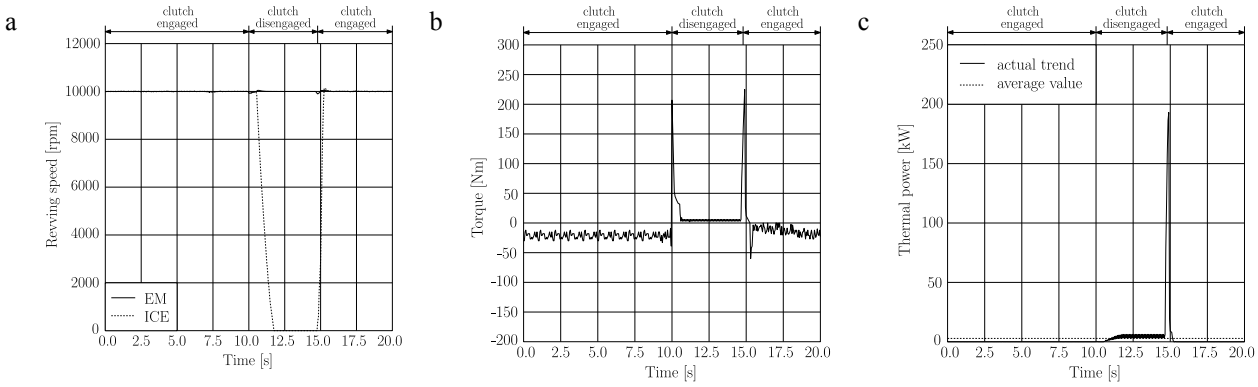

Fig. 4. (a) revving speed of the EM and of the ICE; (b) torque of the EM; (c) thermal power generated by friction.

First, the difference between the revving speed of the ICE and the one of the EM has to be obtained:

$$\Delta speed(t) = |speed_1(t) - speed_2(t)| \tag{1}$$

where $speed_1$ and $speed_2$ are the revving speed of the shaft on the side of the ICE and of the EM respectively, see Fig. 4 (a), and t is the time.

The power generated by friction as a function of temperature, see Fig. 4 (c), can be calculated as follows:

$$\dot{Q}(t) = \Delta speed(t) \cdot Mt_2(t) \tag{2}$$

where $Mt_2(t)$ is the torque registered at point 2, on the side of the EM, see Fig. 4 (b).

The sampling timestep has been 0.01s and considering that the duration of a single cycle is 20s a total of 2000 points have to be managed. Moreover, to have also averaged information along the single cycle, the average heat entering during the test has been derived as follows. First, the total energy, E_{tot} generated during a single cycle has been obtained by adopting the trapezoidal rule (Hildebrand 1987) and then divided by the duration of the single cycle to obtain the average generated heat flux $\dot{Q}_{av}$:

$$E_{tot} = \sum_{i=1}^{2000}[\dot{Q}(t_i) + \dot{Q}(t_{i-1})] \cdot (t_i - t_{i-1}) \cdot \frac{1}{2} \tag{3}$$

$$\dot{Q}_{av} = E_{tot}/t_{cycle} \tag{4}$$

where t_{cycle} is the duration of a cycle (20s).

Concerning the heat exchange with the air surrounding the clutch and favoured by its rotary motion, the formulas proposed by Harmand et al. (Harmand et al. 2013) have been considered:

$$HTC_{air} = (speed_{clutch}/\upsilon_{air})^{0.5} \cdot 0.33 \cdot k_{air} \tag{5}$$

where $speed_{clutch}$ is the regime revving speed of the clutch during the test (10000 rpm), υ_{air} is the kinematic viscosity of air (16.69 mm^2/s) and k_{air} is the conductivity of air (0.00002717 W/(mm°C)).

Regarding the mechanical loadings, the centrifugal load is directly linked to the revving speed and the force applied by the spring to the pressure plate has been provided by the supplier of the cup spring.

4. Finite Element models

Different FE models of increasing complexity have been set up. However, the same types of solid elements have been employed. For both the thermal and structural analyses, tetrahedrons (four nodes, isoparametric, one integration

point), pentahedrons (six nodes, isoparametric, trilinear interpolation function), and hexahedrons (eight nodes, isoparametric, trilinear interpolation function) have been adopted. All the FE simulations have considered one-sixth of the involved components taking advantage of the symmetry of the geometry and loadings. The thermal-structural analyses have been performed adopting a decoupled approach. First, the thermal solution has been computed and, then, imported into the structural model for a more robust modelling strategy.

4.1. FE analysis of the sole structural disc and friction material

This is the simplest model to be implemented and it has been developed in order to understand if a so simplified analysis could be able to grasp the phenomena involved. Only the single clutch disc is considered.

Fig. 5 shows the FE model employed in the analysis. 23000 hexahedral elements have been used. The average mesh size is 0.5 mm and homogeneous along the domain. The region around the notch, where raptures have been detected, has been discretized by adopting a mapped mesh.

The friction material has been connected to the structural disc by nodal continuity to mimic the actual full adhesion condition. To consider the unmodeled components, the heat capacity of the most central portion of the disc has been artificially increased. In particular, it was decided to add the thermal inertia of the spline profiled disc, of the rivets and of the portion of the spline profiled shaft which refers to the considered disc. In this way, a heat capacity of 2630 J/(Kg°C) has been assigned to the central part of the structural disc, see Fig. 5.

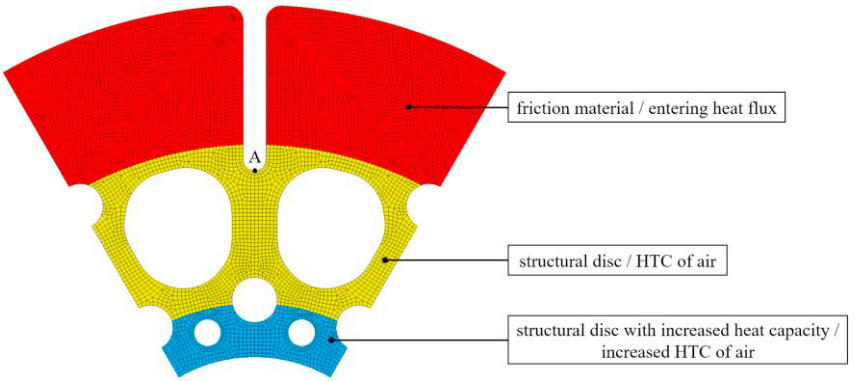

Fig. 5. The first FE model: structural disc and the friction material.

The model has been set up to mimic a warm-up phase of 400s in which the clutch has been engaged and disengaged 20 times. The boundary conditions have included an initial temperature of 37°C measured at the bench at the start of the test, the entering heat flux due to the action of the clutch and a convective exchange with the air in contact by the moving disc. The entering heat flux ($\dot{Q}(t)$) has been applied as specific heat distributed on the faces of the friction material in contact with the steel plates. In addition, it has been necessary to divide this incoming heat by two. In fact, it can be assumed that one half of the heat will be dissipated by the disc and the other half by steel plate through the basket and the flywheel. The heat exchange with air has been modelled with a heat transfer coefficient (HTC) of $7.102 \cdot 10^{-5}$ W/(mm°C) at a temperature of 37°C applied to the external faces of the yellow elements of Fig. 5. Parallelly, an equivalent HTC has been computed in order to artificially take into account the area exposed to the surrounding air belonging to the parts not included in the model and it has been applied to the external faces of the same elements exhibiting the increased heat capacity described before, blue elements of Fig. 5.

Since the heating of the components has to be simulated over time as a consequence of the repeated cycles, a transient analysis is mandatory. To achieve a solution that is as faithful as possible to reality, the same timestep employed for the experimental acquisitions (0.01s) would have been necessary. This calculation revealed itself to be very long, but manageable for this purely thermal calculation. However, this approach becomes unmanageable when thermal-structural numerical forecasts have to be performed, where computational time and file size grow enormously. Therefore, the first step has been to understand whether it is legitimate to approximate the incoming

heat flux of the various repetitive cycles ($\dot{Q}(t)$) to the average one ($\dot{Q}_{av}$ = 0.0378 W/mm^2) to be able to freely choose e higher time step, identical for thermal and thermal-structural analyses, see Fig. 4 (c). So, two simulations have been performed and compared in terms of temperatures. For the sake of brevity, only the results relating to the point at the centre of the notch are reported (point A in Fig. 5). Fig. 6 shows the temperature trend after 20 of the cycles depicted in Fig. 4 (400s of analysis). The fluctuations of the simulation adopting a timestep of 0.01s exhibit a marginal amplitude and oscillate around the value identified by the analysis performed with average thermal power and a higher timestep equal 2s. This graph proves the substantial correctness to ignore the actual profile of the thermal power and, therefore, to consider only its average value. Also, from a thermal-structural point of view, these small oscillations of temperature are usually negligible (Rakopoulos et al. 2004). However, the maximum temperature after 400s settles at 800°C, almost double the value recorded experimentally. This result forces us to carry out more in-depth analyses before approaching a thermal-structural simulation.

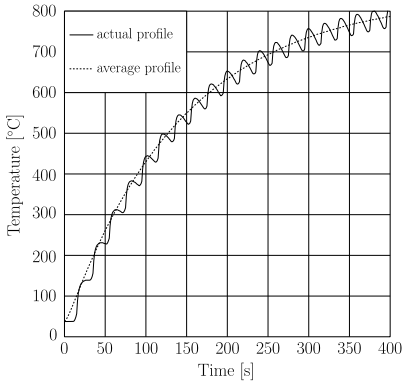

Fig. 6. Comparison of the temperature profile adopting the actual thermal power profile and the average value.

4.2. FE analysis of the whole friction disc and portion of the spline profiled shaft

To understand if the discrepancies between experimental data and numerical forecasts observed employing the simplified model of previous section could be imputable to the adoption of equivalent heat capacity and heat transfer coefficient used to mimic the effects of the unmodeled parts, the model has been enriched by adding these additional components to the analysis. Fig. 7 (a) shows the domain of the analysis: the rivets, the spline profiled disc and a portion of the spline profiled shaft have been added. The model consists of 30000 hexahedral and 200 pentahedral elements. The interactions among the components have been managed by thermal contact. The materials used are friction material and AISI 1060, see Table 1. The same warm-up phase of section 4.1 has been simulated and the same boundary conditions have been applied; note that the surface of convective heat exchange with the surrounding air and the thermal inertia are now fully consistent with the real assembly. Nevertheless, the temperatures in the structural disc in the notch area shown in Fig. 7 (b) are really close to those of the previous case and therefore still too high if compared to the 400°C that has been reached experimentally. This means that the model of Fig. 5 had correctly grasped the thermal inertia of the model of Fig. 7 (a) and also the corrected heat exchange with the air of the central portion of the friction disc had been correctly estimated. Consequently, other effects have to be investigated and a more complex three-dimensional model, involving the whole clutch assembly, has been developed.

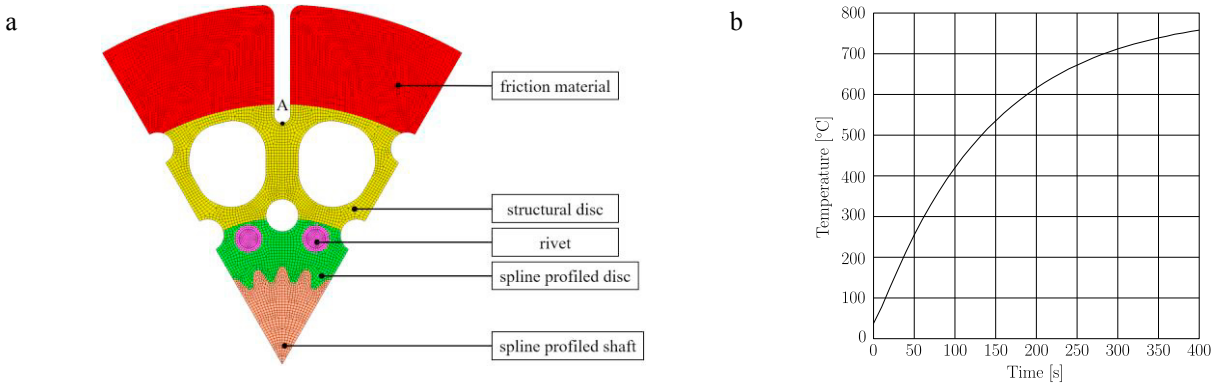

Fig. 7. (a) FE model; (b) temperature profile registered at point A.

4.3. FE analysis of the whole clutch

Fig. 8 shows the model used in these last analyses. A portion of the entire clutch assembly has been modelled by exploiting the symmetry planes. Three friction plates, two steel plates, the pressure plate, the spline profiled shaft, the basket and the flywheel have been considered. 173000 hexahedral elements, 800 pentahedral elements and almost one million tetrahedral elements were employed. All components are made of AISI 1060 except for the friction material.

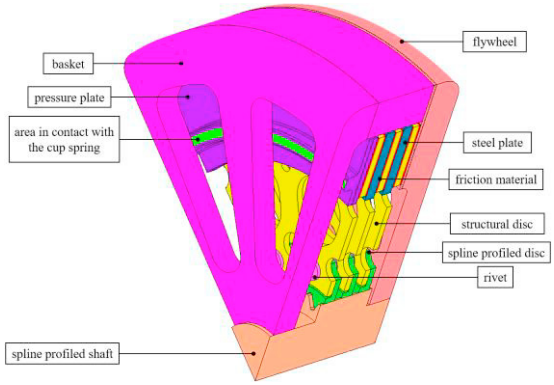

Fig. 8. The FE model of the complete assembly of the clutch.

4.3.1. FE thermal analysis of the whole clutch

At a first stage, this thermal simulation has consisted of the same warm-up phase as the previous simulations.

The same thermal boundaries adopted in the previous cases have been used, but, in this case, all the faces lapped by air of the basket, flywheel and spline profiled shaft have been added. Fig. 9 (a) shows the trend of temperatures as a function of time in the notched area of the three discs: point A' for the disc in contact with the pressure plate, A'' for the disc in the middle and A''' for the disc in contact with the flywheel. The three temperature profiles are essentially coincident. Temperatures reach around 400°C as shown by experimental evidence. This significant drop in temperatures with respect to the previous simplified analysis can be attributed to the absolutely non-negligible effect of the flywheel and basket. Their high inertia and their large heat exchange surface with the air have greatly influenced the maximum temperature reached by the discs. Fig. 9 (b) depicts the whole clutch after 400s, at the end of the first warm-up phase.

Once the thermal warm-up has been validated, the whole thermal cycle has been mimicked and a sequence of warm-ups and cool-downs has been considered. During the warm-up phase, 20 cycles of engage and disengage have been analysed, for a total of 400s. During the cooling-down phases, the clutch has been kept engaged for 800s. To identify the arising of potential hysteresis loops, one warm-up phase followed by a period of cooling down could be sufficient. Nevertheless, two repetitions (first warm-up, first cooldown, second warm-up and second cooldown) have been simulated to confirm the possible arise of stabilized hysteresis loops, see Fig. 9 (c).

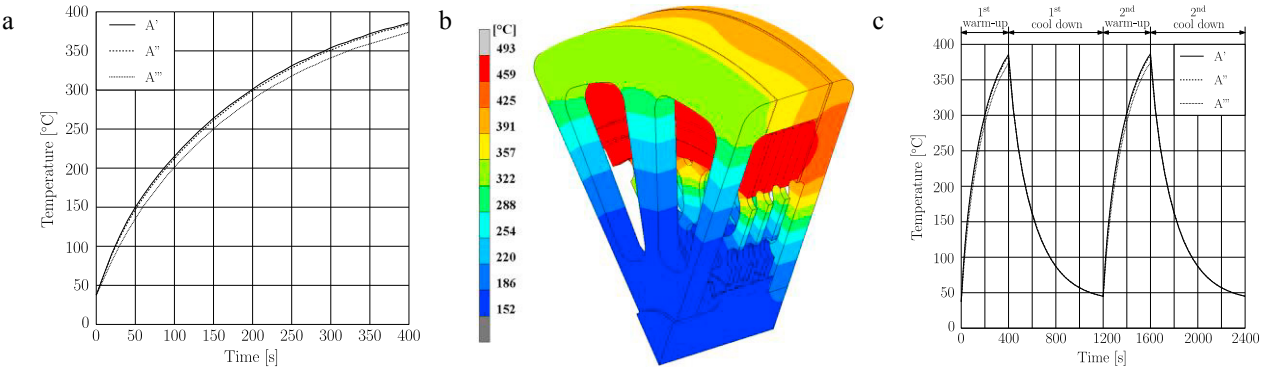

Fig. 9 (a) temperature profile of three structural discs [0-400s]; (b) temperature contour plot of the whole domain after 400s; (c) temperature profile of three structural discs [0-2400s].

4.3.2. FE thermal-structural analysis of the whole clutch

Once a satisfactory thermal calculation has been obtained, a thermo-structural model simulation has been prepared. In this model, the contacts between the various components have been set up. One-sided contacts have been used between the friction materials and the steel plates, pressure plate and flywheel, while glued contacts have been adopted to connect the flywheel and basket and to simulate the effect of rivets. In addition to the effect of temperature, purely mechanical loads have been also superposed. Fig. 8 shows the area of the pressure plate where the spring acts. A pressure of 13 MPa has been assigned to simulate the force of 9000N exerted by the spring. Then the centrifugal force generated by a rotational speed of 10000 rpm has been applied to the entire computational domain. Finally, the appropriate symmetry constraints have been assigned to correctly exploit the sixth of the model used.

For the sake of brevity, the authors have focused only on the analysis of the stress - plastic strain graph which shows the quantities to be monitored to predict the possible occurrence of low-cycle thermal fatigue failure (Sissa et al. 2014). Fig. 10 shows the circumferential stress - plastic strain graph for each of the three nodes at the bottom of the groove of the three clutch discs. Note that two hysteresis cycles have been registered corresponding to the two thermal cycles applied. These three profiles differ slightly in certain areas. These discrepancies could be ascribed to both thermal and structural factors. For instance, Fig. 9 (c) depicts a slight thermal gradient: the disc in contact with the flywheel is the coldest. Additionally, the stiffness of the components in contact with the discs varies. The first disc is pushed by a deformable pressure plate, the third disc is in contact with a very stiff flywheel, and the second disc experiences intermediate stiffness. Therefore, it can be argued that the stiffness of the component in contact with the friction disc has a direct effect on the size of the corresponding hysteresis cycle.

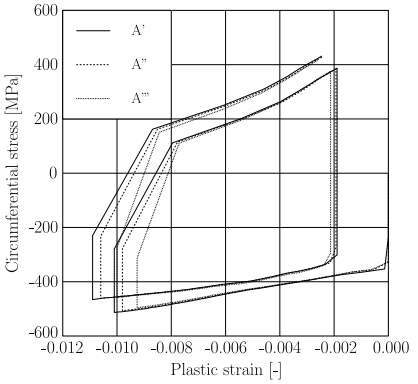

Fig. 10. Circumferential stress – plastic strain curves at points A', A'' and A'''.

5. Conclusions

This contribution has shown a methodology for the thermal-structural calculation of a P2-type hybrid powertrain clutch. The analyzed assembly showed cracks in a particularly unfavourable area of the structural discs, prompting the need for an explanation. The process of deriving boundary conditions from experimental data was explained in detail, followed by the development of increasingly complex numerical models. The first model consisted of just one structural disc and friction material but was too simplified and showed temperatures almost double compared to experimental data. A second, more accurate model was then created by adding the rivets, the spline profiled disc, and a portion of the spline profiled shaft. However, even this model failed to achieve temperatures in line with the experimental data. A third and final model was developed, incorporating the three friction discs, two steel plates, pressure plate, flywheel, basket, and spline profiled shaft. A thermal analysis was carried out, leading to satisfactory results, and a thermal-structural analysis was performed, revealing the arise of plastic hysteresis loops in the notched areas of the structural discs, and explaining the observed low cycle fatigue failures. These results indicate that a more comprehensive approach is necessary, and possible well design guidelines may include redesigning the clutch to reduce temperatures and stresses or adopting a specific set-up of the control unit to limit repeated usages and give the clutch time to cool down.

References

Abdullah, O. I., Schlattmann, J., Majeed, M. H., Sabri, L. A., 2019. The distribution of frictional heat generated between the contacting surfaces of the friction clutch system. International Journal on Interactive Design and Manufacturing (IJIDeM) 13, 487–498.

Afferrante, L., Decuzzi, P., 2004. The effect of engagement laws on the thermomechanical damage of multidisk clutches and brakes. Wear 257, 66–72.

Barbieri, S. G., Mangeruga, V., Giacopini, M., Callegari, M. S., Bagnoli, L., 2023. The Effect of the Thermal Mean Stress Value on the Vibration Fatigue Assessment of the Exhaust System of a Motorcycle Engine. SAE International Journal of Engines, in press.

Chaboche, J. L., 1986. Time-independent constitutive theories for cyclic plasticity. International Journal of Plasticity 2, 149–188.

Chaboche, J. L., 1989. Constitutive equations for cyclic plasticity and cyclic viscoplasticity. International Journal of Plasticity 5, 247–302.

Chaboche, J. L., 2008. A review of some plasticity and viscoplasticity constitutive theories. International Journal of Plasticity 24, 1642–1693.

Charkaluk, E., Bignonnet, A., Constantinescu, A., Dang Van, K., 2003. Fatigue design of structures under thermomechanical loadings. Fatigue & Fracture of Engineering Materials & Structures 26, 661–661.

Constantinescu, A., Charkaluk, E., Lederer, G., Verger, L., 2004. A computational approach to thermomechanical fatigue. International Journal of Fatigue 26, 805–818.

Della Gatta, A., Iannelli, L., Pisaturo, M., Senatore, A., Vasca, F., 2018. A survey on modeling and engagement control for automotive dry clutch. Mechatronics 55, 63–75.

Foulard, S., Rinderknecht, S., Ichchou, M., Perret-Liaudet, J., 2015. Automotive drivetrain model for transmission damage prediction. Mechatronics 30, 27–54.

Harmand, S., Pellé, J., Poncet, S., Shevchuk, I. V., 2013. Review of fluid flow and convective heat transfer within rotating disk cavities with impinging jet. International Journal of Thermal Sciences 67, 1–30.

Hildebrand, F. B., 1987. Introduction to Numerical Analysis second ed. Dover Publications, New York, NY.

Ivanović, V., Herold, Z., Deur, J., Hancock, M., Assadian, F., 2009. Experimental Characterization of Wet Clutch Friction Behaviors Including Thermal Dynamics. SAE International Journal of Engines 2, 2009-01–1360.

Lorenzini, M., Giacopini, M., Barbieri, S. G., 2018. Thermo-Mechanical Analysis of the Exhaust Manifold of a High Performance Turbocharged Engine. Key Engineering Materials 774, 307–312.

Mangeruga, V., Giacopini, M., Barbieri, S. G., Berni, F., Mattarelli, E., Rinaldini, C., 2019. Design of a Hybrid Power Unit for Formula SAE Application: Packaging Optimization and Thermomechanical Design of the Electric Motor Case. SAE Technical Paper Series, Vol.2019.

Mangeruga, V., Giacopini, M., Barbieri, S., Russo, M., 2020. Investigation on the Dynamic Behaviour of a Torque Transmission Chain for an Innovative Hybrid Power Unit Architecture. SAE Technical Papers, Vol. 2020.

Mangeruga, V., Renso, F., Raimondi, F., Giulio, S., Giacopini, M., 2023a. Influence of the Crankshaft Dynamic Phenomena on the Fatigue Behaviour of a Transmission Chain in a Hybrid Power Unit. AIP Conference Proceedings, in press.

Mangeruga, V., Renso, F., Barbieri, S. G., Giacopini, M., Raimondi, F., 2023b. Investigation of the Dynamic Effects on the Fatigue Behaviour of a Transmission Chain in a Hybrid Power Unit. Journal of Multiscale Modelling, in press.

Mattarelli, E., Rinaldini, C. A., Scrignoli, F., Mangeruga, V., 2019. Development of a Hybrid Power Unit for Formula SAE Application: ICE CFD-1D Optimization and Vehicle Lap Simulation. SAE Technical Paper Series, Vol. 2019 , pp. 1–51.

Minh, V. T., Mohd Hashim, F. B., Awang, M., 2012. Development of a real-time clutch transition strategy for a parallel hybrid electric vehicle. Proceedings of the Institution of Mechanical Engineers, Part I: Journal of Systems and Control Engineering 226, 188–203.

Pavković, D., Cipek, M., Plavac, F., Karlušić, J., Krznar, M., 2022. Internal Combustion Engine Starting and Torque Boosting Control System Design with Vibration Active Damping Features for a P0 Mild Hybrid Vehicle Configuration. Energies 15, 1311.

Rakopoulos, C. D., Rakopoulos, D. C., Mavropoulos, G. C., Giakoumis, E. G., 2004. Experimental and theoretical study of the short term response temperature transients in the cylinder walls of a diesel engine at various operating conditions. Applied Thermal Engineering 24, 679–702.

Sissa, S., Giacopini, M., Rosi, R., 2014. Low-cycle thermal fatigue and high-cycle vibration fatigue life estimation of a diesel engine exhaust manifold. Procedia Engineering 74, 105–112.

Sivanesan, M., Jayabalaji, G., 2017. Modelling, Analysis and Simulation of Clutch Engagement Judder and Stick-Slip. SAE International Journal of Passenger Cars - Mechanical Systems 10, 54–64.

Steinhagen, H. G., 1980. The Plate Clutch. SAE Technical Papers , Vol. 89pp. 3097–3119.

Wang, S., Kersting, T., Rohe, M., Pennec, B., 2016. Concept solution for efficiency improvement of a powertrain with P2 hybrid technology by an intelligent hybrid control unit 1131–1142.